Journal of ELECTRONIC MATERIALS, Vol. 38, No. 12, 2009
DOI: 10.1007/s11664-009-0913-1
© 2009 TMS
Special Issue Paper

Nonuniform and Negative Marker Displacements Induced by Current Crowding During Electromigration in Flip-Chip Sn-0.7Cu Solder Joints

S.W. LIANG,[1] HSIANG-YAO HSIAO,[1] CHIH CHEN,[1,4] LUHUA XU,[2] K.N. TU,[2] and YI-SHAO LAI[3]

1.—Department of Material Science and Engineering, National Chiao Tung University, Hsin-chu 30010, Taiwan, ROC. 2.—Department of Materials Science and Engineering, UCLA, Los Angeles, CA 90095-1595, USA. 3.—Central Laboratories, Advanced Semiconductor Engineering, Inc., Kaohsiung 811, Taiwan, ROC. 4.—e-mail: chih@mail.nctu.edu.tw

A quantitative analysis of the nonuniform distribution of current density and nonuniform rate of electromigration has been carried out by measuring the movement of an array of diffusion markers. Tiny marker arrays were fabricated by focused ion beam on the polished surface of flip-chip solder joints near the anode to measure the electromigration rate. The marker velocity at the current-crowding region was found to be at least five times larger than at locations far from the region. Some of the markers in the low-current-density region possess negative velocities, indicating that backflow occurs during the electromigration. The backflow, in which the atomic flow is against the electron flow, is explained by a constant-volume model as well as the back-stress induced by electromigration.

Key words: Electromigration, Pb-free solder

INTRODUCTION

Flip-chip solder joints in future high-performance electronic products may carry electric current densities above 1×10^4 A/cm^2.[1,2] Due to the unique line-to-bump geometry, current crowding occurs when the current enters the solder bump from the traces on the chip side. By using the finite-element method to simulate current distribution, it was found that the current density in the current-crowding area can be one order of magnitude higher than the average density in the solder bump.[3,4] The effect of current crowding on pancake-type void formation at the cathode and whisker growth at the anode of solder joints has been reported.[5–7] However, the effect of nonuniform distribution of electric current on diffusion in the bulk of the solder bump is unclear, and no direct measurement of the rate of electromigration in the current-crowding region versus that in the rest of the solder bump has been reported. In this paper, diffusion markers prepared by focused ion beam (FIB) were used to measure the nonuniform distribution of diffusion flux in the solder joint during electromigration. The distribution of movement of markers is found to be in direct proportion to the local current density distribution. However, atomic flow against electron flow in the low-current-density region has been observed. The product DZ^*, the diffusivity times the effective charge number, in the current-crowding region has been estimated.

(Received February 25, 2009; accepted July 24, 2009; published online August 13, 2009)

EXPERIMENTAL PROCEDURES

To observe the effect of current crowding in electromigration, flip-chip solder joints with thin-film underbump metallization (UBM) were adopted. The test vehicles were 13 mm × 10 mm × 0.56 mm flip-chip packages with a 3.5 mm × 0.5 mm × 0.73 mm silicon chip interconnected to a substrate. The pitch between adjacent solder joints was 270 μm.

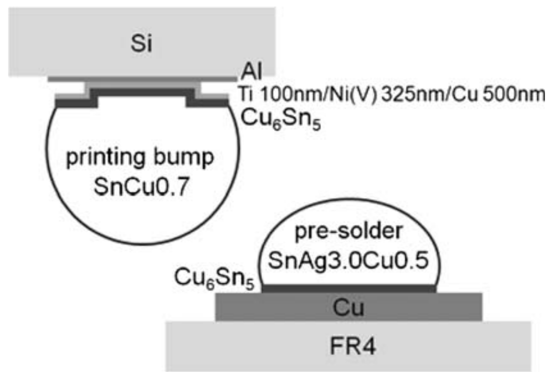

Fig. 1. Schematics for the flip-chip solder adopted in this study.

The UBM is a trilayer metallization of Ti 100 nm/ Ni(V) 325 nm/Cu 500 nm. The diameters of the UBM opening and the passivation opening of the UBM were 110 μm and 85 μm, respectively. Sn-0.7Cu solder was printed on the chip side. The substrate pad metallization features the solder-on-pad (SOP) surface treatment, i.e., with printed Sn-3.0Ag-0.5Cu presolder on the Cu pad surface, as shown schematically in Fig. 1. The printed solder and the SOP were reflowed together to become lead-free solder bumps.

SIMULATION

Three-dimensional finite element analysis was employed to simulate the current density distribution in the solder joints. The model included two solder joints, an Al trace, and two Cu lines, as shown in Fig. 2a. The direction of the electron current is shown in Fig. 2a by the arrows. The dimensions of the Al trace, pad opening, and the Cu line were identical to those of the real flip-chip sample. The intermetallic compound (IMC) formed between the UBM and the solder was also considered in the simulation models. It is assumed that 0.5 μm of the Cu layers on the chip and the substrate sides are consumed and that a thickness of 2.0 μm of Cu_6Sn_5 IMC was formed. Layered IMCs were used in this simulation for the Cu_6Sn_5 to avoid meshing difficulties. Moreover, the trilayered UBM was simplified as a one-layer structure in the model. In addition, Sn-0.7Cu solder was used in this model. The resistivity values of the materials used in the simulation are listed in Table I. The model used in this study was based on ANSYS simulation software with SOLID5 eight-node hexahedral coupled field elements. The size of the element in the solder bump was between 0.5 μm and 1.0 μm as illustrated in Fig. 2b. Such a high density of elements will make the simulation results close to the real current distribution.

RESULTS AND DISCUSSION

The sample was polished approximately to the centers of the solder bumps. To avoid thermomigration during electromigration tests,[8,9] a low

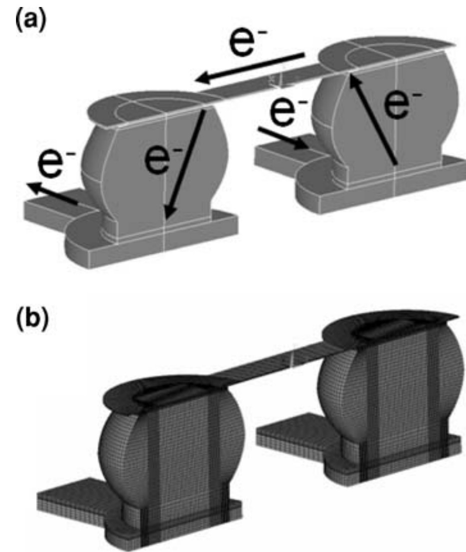

Fig. 2. (a) The simulation model for one pair of flip-chip solder joints; arrows show the direction of the electron current. (b) The mesh of the simulation model; each element size is about 0.5 μm to 1.0 μm.

current density was used to induce void formation. A current of 0.6 A was applied to one pair of solder joints on a hotplate maintained at 100°C. At the very beginning of electromigration, infrared (IR) microscopy was used to measure the temperature distribution in the bump. The temperature distribution is illustrated in Fig. 3. The bump on the left-hand side, denoted bump 1, was subjected to downward electron current stressing. The temperature distribution is quite uniform, as shown in Fig. 3a. No clear hot-spots were found in the bump. Figure 3b shows the temperature profile from point A to point B as marked in Fig. 3a. No obvious thermal gradient across the bump was exhibited. Accordingly the result from IR microscopy indicated that no large thermal gradient was created under current stressing with 0.6 A at 100°C. Therefore, we concluded that thermomigration does not accompany electromigration in the test.

To correlate qualitatively the current crowding to the electromigration flux in the solder joint, marker analysis was used to measure the nonuniform distribution of electromigration flux. Twelve markers were fabricated by FIB; each marker was a square of 1 μm $\times$ 1 μm and was 200 nm in depth. The pitch of the marker array was 10 μm. The distance between the marker and the contact interface to the Si die was about 11 μm to 12 μm. Figure 4 shows scanning electron microscopy (SEM) images of the markers after various stressing times. Figure 4a shows the image before current stressing. In the electromigration test, the electron flow was coming from the upper-right corner of Fig. 4a. After stressing for 150 h, the formation of IMCs near the upper-right corner became clear, as shown in Fig. 4b. The tin atoms have moved to the anode side due to electromigration. After stressing for 300 h,

Table I. The Properties of Materials Used in the Simulation Model

Materials	Resistivity at 20°C ($\mu\Omega$ cm)
Al trace	3.2
Ti/Ni(V)	58.4
Cu lines	1.7
Cu_6Sn_5	17.5
Sn-0.7Cu solder	12.3

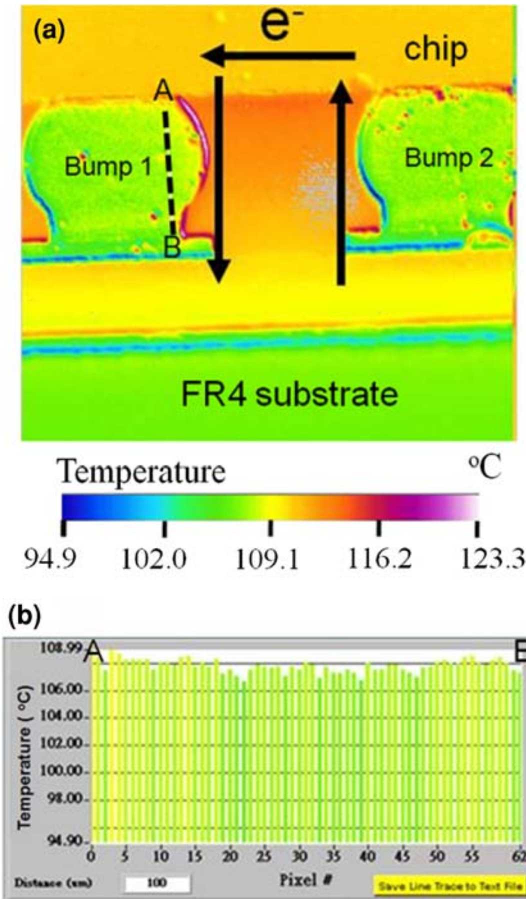

Fig. 3. (a) IR images showing the temperature distribution in the bump with current stressing of 0.6 A at 100°C. (b) Temperature profile along the dashed line in the bump.

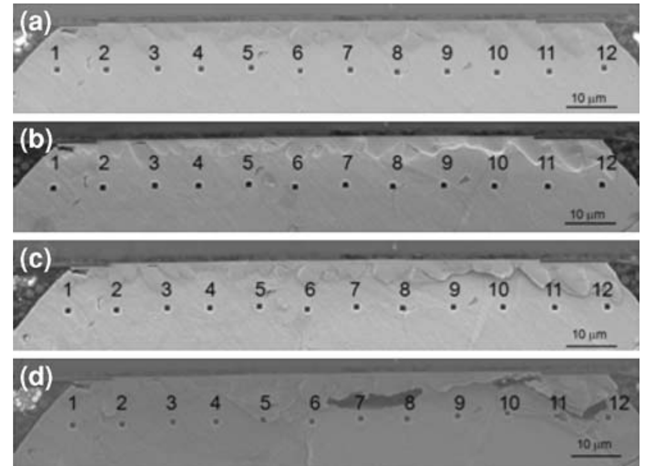

Fig. 4. SEM images of the solder before and after current stressing for: (a) 0 h, (b) 150 h, (c) 300 h, and (d) 1632 h.

when we compared the markers at the right corner with those at the left corner, the movement of marker no. 10 became clearer, as shown in Fig. 4c. It moved closer to the die. After 1632 h of current stressing, voids formed at the cathode end, as shown in Fig. 4d. Some IMCs disappeared near the anode entrance of the Cu trace on the substrate, and voids formed between the IMC and solder on the cathode side.

To obtain the quantitative analysis of current density and marker movement, the three-dimensional (3-D) current density distribution was constructed using the finite-element method and the marker movement was measured from the SEM image. In Fig. 5a and b, current crowding is shown to occur at the upper-right region, near the exit point of the Al interconnect. The average current density is about 1.26×10^4 A/cm^2 on the basis of the UBM opening, but the maximum current density is 9.53×10^4 A/cm^2 in the solder bump, adjacent to the UBM. Figure 5c shows the current density distribution corresponding to the marker position. Indeed, the current-crowding effect occurred close to marker no. 10. The current density at marker no. 10 reached 4.8×10^4 A/cm^2, which is slightly lower than the maximum current density, because it was about 11 μm away from the die. The average current density on the UBM opening is 1.26×10^4 A/cm^2. The current-crowding ratio, denoted by the maximum current density divided by the average current density, is about 3.8. The current density away from the current exit point is smaller than 1×10^4 A/cm^2.

To observe the marker movement, the positions of markers were measured before and after current stressing. The software used can translate the pixels in the SEM image into length. The uncertainty is estimated to be about 0.1 μm. The evolution of the marker positions is shown in Fig. 6a. It was found that the markers near the current-crowding region (nos. 6–10) moved close to the Si die. Since the electron flow went from the chip side to the substrate side, the Sn atoms were pushed downward and the vacancies were pushed upward. However, the marker movement at the low-current-density region (nos. 1–5) was in the opposite direction, against the electron flow. This interesting phenomenon will be discussed later. The markers almost did not move horizontally. The depths of the markers were not measured, although the marker depth may change after electromigration. It is believed that the markers move mainly in the vertical direction, i.e., the direction of electron flow, so the

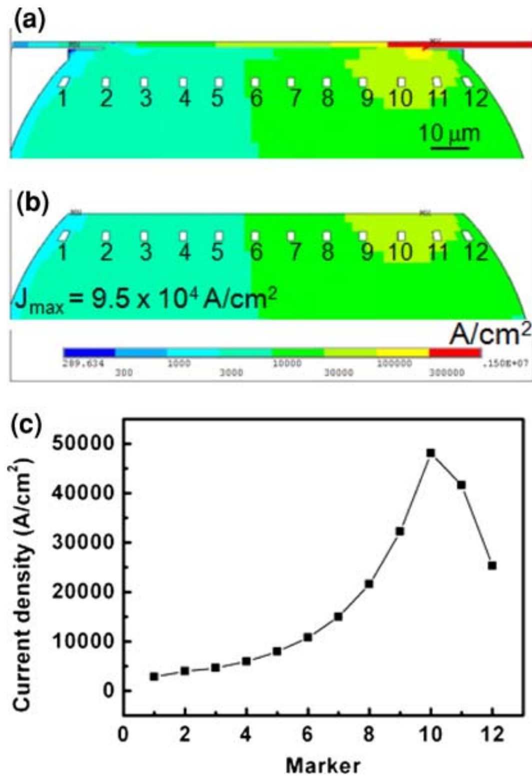

Fig. 5. Simulation results for the current density distribution in the flip-chip solder joints: (a) with Al trace and UBM, (b) with the solder bump only, and (c) local current density at the 12 marker positions.

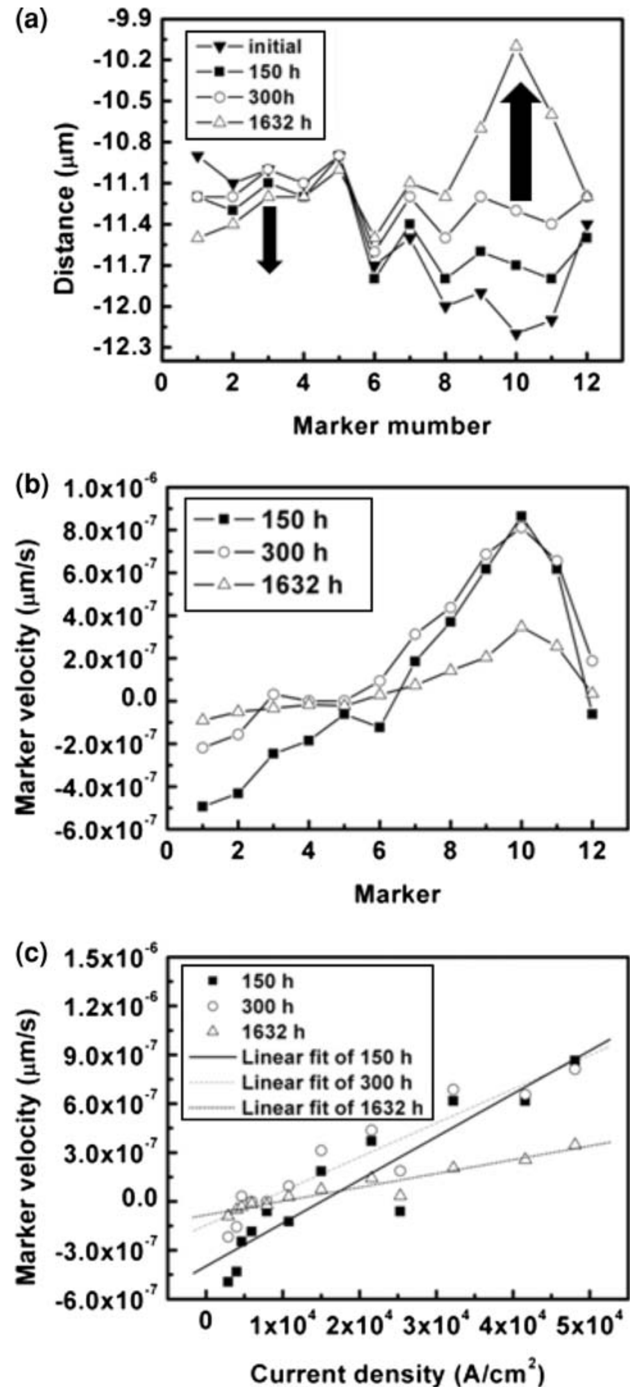

Fig. 6. (a) Evolution of position for the 12 markers at various stressing times. (b) Marker velocity at the 12 positions for different stressing times. (c) Plot of marker velocity as a function of local current density for different stressing times. The marker velocity is proportional to the local current density at the marker.

marker movement in the other two directions can be ignored. To determine the velocity of marker movement, we define it as the difference in distance between the edge of the Si die and the marker before and after current stressing divided by the stressing time. As shown in Fig. 6b, for 150 h and 300 h current stressing, it is clear that the largest marker movement is for marker no. 10. The other markers have lower velocities. These results prove the effect of current crowding experimentally. After 1632 h of current stressing, the maximum marker velocity still occurred for marker no. 10. However, the velocity of marker no. 10 decreased from 8.6×10^{-7} μm/s to 3.5×10^{-7} μm/s. Since the current-crowding region has the highest atom diffusion velocity, void formation and propagation started from the entrance point of the Al interconnect. After the pancake-type void formed, the conducting path was interrupted, forcing the conduction to pass around the void. Thus, the velocity of markers near the original current-crowding region decreased, whereas the velocity away from the current-crowding region increased. We note that the markers in low-current-density regions (nos. 1–5) possess negative velocities.

It has been reported that the threshold current density for electromigration in pure Sn is about 8×10^3 A/cm^2 at 100°C.[10] The local current densities at markers 1–5 may be lower than the threshold current densities. Thus, in these regions no electromigration occurred and no back-stress was induced. However, the negative marker velocities indicate that atomic flow has occurred, but against the electron flow. Such migration may occur if we assume a constant volume of the solder bump.

In the high-current-density region, atoms are driven to the anode. There, back-stress develops as accumulation occurs. When the stress exceeds the elastic limit, either plastic deformation or lattice shift occurs to relieve the stress. If we assume a constant-volume model, the anode needs to create room for the incoming atomic flux by outdiffusion. The outdiffusion can occur under a stress gradient going from the high-back-stress region to the neighboring low-back-stress region. Then, the lattice shift of atomic back-flow occurs in the low-current-density region because the resistance is lower. As a consequence, we have negative marker motion in the low-current-density region.

In Fig. 6c, we obtain a direct correlation between current density distribution and marker velocity distribution in the solder joint. For electromigration in Al films, it has been shown that the relationship is linear if the current density is low.[11–13] In the presented results, the lines fitted to the data at both 300 h and 1632 h show a linear relationship between current density and marker velocity, indicating that reliable data have been obtained in this study. In addition, it is noteworthy that the measured velocity varied with the stressing time. This may be attributed to the following two reasons. First, there exists an incubation time for electromigration. Thus, the measured velocities for the three stressing times are not constant. Second, the local current densities at the markers may change with time due to the formation of voids or other defects in the solder.

Under electromigration, the electron wind force and back-stress gradient induced atomic fluxes are given as[14]:

$$J_{\mathrm{em}} = C\frac{D}{kT}Z^{*}eE - C\frac{D}{kT}\frac{\mathrm{d}\sigma\Omega}{\mathrm{d}x}, \tag{1}$$

where J_{em} is the atom flux in unit of atoms/cm^2 s, C is the concentration of atoms per unit volume, D/kT is the atomic mobility, σ is the hydrostatic stress in the metal, $\mathrm{d}\sigma/\mathrm{d}x$ is the stress gradient along the direction of electron flux, Ω is the atomic volume, Z^* is the effective charge number of electromigration, e is the electron charge, and E is the electric field. In this study, the electromigration was focused in the current-crowding region at the cathode end. When we take Ω_{Sn} to be 2.71×10^{-29} m^3, $\Delta\sigma$ to be about 20 MPa, and Δx to be 75 μm, the back-stress gradient is several orders of magnitude smaller than the electron wind force. The estimated electromigration and back-stress fluxes are about 75°C atoms/cm^2 s and 0.45°C atoms/cm^2 s, respectively. Thus, the back-stress is negligible here. Equation 1 can be rewritten as:

$$J_{\mathrm{em}} = C\frac{D}{kT}Z^{*}eE = C\langle v\rangle \tag{2}$$

where $\langle v\rangle$ is the atomic drift velocity, and $E = \rho j$, where ρ is the metal resistivity and j is the electron current density. Then, the mean atomic drift velocity $\langle v\rangle$ in electromigration is given by

$$\langle v\rangle = \frac{eDZ^{*}}{kT}\rho j. \tag{3}$$

Here, T is 108°C, which is equal to the value of 381 K measured by IR microscopy, ρ is 16 $\mu\Omega$ cm at this temperature according to the temperature coefficient of resistivity of the solder. From the results shown in Fig. 4, DZ^* was calculated from each marker position by using this equation. The average DZ^* was calculated to be 3.3×10^{-12} cm^2/s. The lattice diffusivities in pure β-Sn along the direction parallel and normal to the c-axis are 1.6×10^{-14} cm^2/s and 3.8×10^{-14} cm^2/s, respectively.[15] Therefore, the average D of tin in tin is 2.7×10^{-14} cm^2/s at 108°C; the calculated value of Z^* is 125, which is high but not unreasonable. Tsai et al. calculated DZ^* for eutectic Sn-Pb to be 5.0×10^{-10} cm^2/s.[16] So, DZ^* of the lead-free solder is two orders of magnitude lower than that of eutectic Sn-Pb under the same temperature. It is most likely that the diffusivity in eutectic Sn-Pb is much higher than that in eutectic Sn-Cu.

CONCLUSIONS

The distribution of electromigration rate in flip-chip solder joints was measured by an array of markers near the cathode end. We found that the electromigration rate at the current-crowding region was much higher than for the rest of the solder joint, which supports the previous simulation results on the effect of current crowding. The nonuniform electromigration resulted in nonuniform and even negative marker motion. The latter indicates a back-flow of atomic flux. We have proposed a constant-volume model and back-stress to explain this. In addition, DZ^* for Sn-0.7Cu solder was calculated to be about 3×10^{-12} cm^2/s.

ACKNOWLEDGEMENTS

The authors at NCTU would like to thank the National Science Council of ROC for the financial support through Grant Nos. NSC96-2628-E-009-010-MY3 and NSC-096-2917-I-009-107. The authors at UCLA would like to acknowledge support from The Seoul Technopark, South Korea.

REFERENCES

1. K.N. Tu, *J. Appl. Phys.* 94, 5451 (2003).
2. *International Technology Roadmap for Semiconductors, Assembly and Packaging Section* (Semiconductor Industry Association San Jose, CA, 2003), pp. 4–9.
3. E.C.C. Yeh, W.J. Choi, K.N. Tu, P. Elenius, and H. Balkan, *Appl. Phys. Lett.* 80, 580 (2002).
4. T.L. Shao, S.W. Liang, T.C. Lin, and C. Chen, *J. Appl. Phys.* 98, 044509 (2005).
5. J.W. Nah, K.W. Paik, J.O. Suh, and K.N. Tu, *J. Appl. Phys.* 94, 7560 (2003).
6. L.Y. Zhang, S.Q. Ou, J. Huang, K.N. Tu, S. Gee, and L. Nguyen, *Appl. Phys. Lett.* 88, 012106 (2006).

7. Y.W. Chang, S.W. Liang, and C. Chen, *Appl. Phys. Lett.* 89, 032103 (2006).
8. H.-Y. Hsiao, S.W. Liang, M.-F. Ku, C. Chen, and D.-J. Yao, *J. Appl. Phys.* 104, 033708 (2008).
9. S.H. Chiu, T.L. Shao, C. Chen, D.J. Yao, and C.Y. Hsu, *Appl. Phys. Lett.* 88, 022110 (2006).
10. H.C. Yu, S.H. Liu, and C. Chen, *J. Appl. Phys.* 98, 013540 (2005).
11. H.B. Huntington and A.R. Grone, *J. Phys. Chem. Solids* 20, 76 (1961).
12. I.A. Blech, *Appl. Phys. Lett.* 29, 131 (1976).
13. I.A. Blech, *Acta Mater.* 46, 3717 (1998).
14. L. Xu, J.H.L. Pang, and K.N. Tu, *Appl. Phys. Lett.* 89, 221909 (2006).
15. K.N. Tu, *Solder Joint Technology: Materials, Properties, and Reliability* (New York: Springer, 2007), Chapter 6, p. 175.
16. C.M. Tsai, Y.S. Lai, Y.L. Lin, C.W. Chang, and C.R. Kao, *J. Electronic Mater.* 35, 1781 (2006).